Identification of miRNA-mRNA Interaction in Vero Cells after Infection of SADS-CoV through Integrative Transcriptome Analysis

Yaoyao Zheng[1,2], Jiaoling Wu[1,2], Yuqi Chen[1,2], Xiaoyu Tang[1,2], Yaorong Tan[1,2], Yuan Sun[1,2], Qianniu Li[1,2], Ruiting Wu[1,2], Xiangbin Zhang[1,2,*] and Jingyun Ma[1,2,*]

[1]*College of Animal Science, South China Agricultural University, Guangzhou, China*

[2]*Key Laboratory of Animal Health Aquaculture and Environmental Control, Guangzhou, Guangdong, China*

Abstract: Swine acute diarrhea syndrome coronavirus (SADS-CoV) is a novel coronavirus that can cause severe diarrhea in newborn piglets in China. Here, we reported profiles of differentially expressed miRNAs and mRNAs in Vero cells infected by SADS-CoV. In total, 345 miRNAs and 1014 mRNAs were identified with significantly differential expression after SADS-CoV infection. The analysis of miRNA-mRNA-pathway network indicated that through major mRNA nodes, TUBA, KRAB, eIF4E and SIRPA_B1_G, differentially expressed miRNAs were mainly involved in pathways of pathogenic Escherichia coli infection, apoptosis, PI3K-Akt signaling pathway, focal adhesion and so on. The qRT-PCR validation results of six selected genes were concordant with RNA-Seq results. This study is the first report to examine differentially expressed miRNAs and mRNAs after SADS-CoV infection in Vero cells, which may help elucidate the underlying mechanisms of SADS-CoV infection.

Keywords: SADS-CoV, Vero cells, Differentially expressed miRNA, Differentially expressed mRNA, miRNA-mRNA-pathway network.

INTRODUCTION

Swine acute diarrhea syndrome coronavirus (SADS-CoV), a novel coronavirus, was first discovered in Southern China in January 2017. SADS-CoV was isolated from intestinal and faecal samples of neonatal piglets with severe watery diarrhea at that time, and it caused the death of 24,693 piglets in four farms of Guangdong Province. During the next four months, that resulted in great losses in the field of pig industry [1-3]. A retrospective investigation revealed that SADS-CoV emerged in China at least since August 2016 and had a high co-infection rate with the most common pig diarrhea virus, porcine epidemic diarrhea virus (PEDV) [4]. Currently, SADS-CoV was isolated from Fujian Province, and remerged in Guangdong Province [5, 6]. It is urgent to understand more about the pathogenic mechanisms of SADS-CoV to prevent its further transmission in China.

MicroRNAs (miRNAs) are small ~23nt RNAs that are considered to play important gene-regulatory roles in animals and plants [7]. In recent years, research has showed that miRNA is a key regulator of virus-host interaction and has become a hot topic nowadays. PEDV, similar to SADS-CoV, is a coronavirus that causes persistent diarrhea in pigs. The infection of PEDV had a significant impact on the level of miRNA expression in PK-15 cells [8]. It was pointed out that miR-221-5p could inhibit PEDV replication by targeting the 3' UTR of the viral genome and activating the NF-kappa B signaling pathway [9, 10]. Research showed that *in vivo* infection with transmissible gastroenteritis virus (TGEV) could reduce the expression level of miR-30a-5p in the ileum of piglets, but significantly increased suppressor of cytokine signaling protein 1 (SOCS1) and suppressor of cytokine signaling protein 3 (SOCS3) expressing, which further dampened the Interferon-I (IFN-I) antiviral response and facilitated viral replication [11]. The miR-22 could promote the activation of NF-kappa B pathway by binding ssc_circ_009380 during TGEV-induced inflammation [12]. Other findings showed that miR-4331 could aggravate TGEV-induced mitochondrial damage by repressing the expression of Retinoblastoma 1 (RB1), and promoting interleukin-1 receptor accessory protein (IL1RAP) expression to activate p38 MAPK pathway [13]. And miR-27b could attenuate apoptosis induced by TGEV infection via targeting runt-related transcription factor 1 (RUNX1) [14]. Previous research indicated that let-7f-5p significantly inhibited the replication of porcine reproductive and respiratory syndrome virus (PRRSV) through suppressing the expression of non-muscle myosin heavy chain 9 (MYH9) [15]. While miR-22 or miR-24-3p could facilitate PRRSV replication by dampening heme oxygenase-1 (HO-1) expression [16, 17]. Taken together, studies on microRNA-mRNA regulatory

*Address correspondence to these authors at the College of Animal Science, South China Agricultural University, Tianhe District, Wushan Road 483, Guangzhou, 510642, China; E-mail: majy2400@scau.edu.cn

College of Animal Science, South China Agricultural University, Tianhe District, Wushan Road 483, Guangzhou, 510642, China;
E-mail: zhangxb@scau.edu.cn

E-ISSN: 2310-0796/20

network have provided information on the mechanisms of virus infection, which would give valuable information for virus control.

In the present study, differentially expressed miRNAs and mRNAs in SADS-CoV inoculated Vero cells were firstly analyzed by RNA sequencing (RNA-Seq) to identify the role of miRNAs SADS-CoV infection mechanism, which would provide a new insight for the pathogenic mechanisms of SADS-CoV.

MATERIALSANDMETHODS

Cell Culture and SADS-CoV Infection

African green monkey kidney cells (Vero cells) were kept in our laboratory and cultured in Dulbecco's Modified Eagle Medium (DMEM, Gibco) supplemented with 10% fetal bovine serum (FBS, Gibco) at a humidified incubator under the condition of 37 °C with 5% CO_2. The virus strain SADS-CoV/CN/GDWT/2017 (GenBank accession number MG557844) was isolated and preserved in our laboratory. When the confluence of monolayer cells reaching approximately 80%, cells were washed twice with DMEM, then mock-infected or infected by SADS-CoV at a dose of 1.0multiplicity of infection (MOI). After inoculation, cells were cultured in serum-free medium containing 8 μg/mL Trypsin-EDTA (Thermo Fisher Scientific, Gibco) at the same conditions mentioned above for 1 hour, and then the medium was replaced by DMEM with 8 μg/ mL Trypsin-EDTA. At the early stage of 4 hours post infection (4hpi), the middle stage (8hpi) and the late stage (16hpi), samples were collected respectively, and were tested in triplicate.

RNA Extraction, Preparation and Sequencing of cDNA Library

Total RNA was extracted with the TRIzol kit (Invitrogen, USA) following the manufacturer's instructions. The purity and concentration of extracted RNA were detected by Nanodrop2000 (IMPLEN, CA, USA).The RNA quality was verified using a 2100 Bioanalyzer (Agilent Technologies,Santa Clara, CA) and also checked by RNase free agarose gel electrophoresis.

Equal amounts of total RNA of mock-infected or infected cells at three time points were pooled for the construction of cDNA libraries. The cDNA libraries of mRNA were constructed by using a TruSeq^{TM} Stranded Total RNA Library Prep Kit (Illumina, USA). Next, ribosomal RNA was removed using Ribo-Zero Magnetic Kit (EpiCentre, USA). All mRNA was broken into ~200bp fragments by adding fragmentation buffer. The first-strand cDNA was obtained by using random primer through reverse transcription. The second-strand cDNA was added End Repair Mix and bases "A" for ligating to adaptor. Then, the second-strand cDNA was digested by the enzyme UNG. Finally, the first-strand cDNA library was sequenced on Hiseq sequencing plamform (Illumina Hiseq 2000). The libraries of miRNA were constructed by using TruSeq^{TM} Small RNA sample prep Kit (Illumina, USA). All other steps were performed according to manufacturer's protocols. A selected clean reads were obtained by removing low quality sequences which were determined by Q20, Q30 and GC content. SeqPrep (https://github.com/jstjohn/SeqPrep), Sicklele (https://github.com/najoshi/sickle) and Fastx-Tollkit (http://hannonlab.cshl.edu/fastx_toolkit/) were used to analyze the clean data. The sequences were analyze using Hisat2 (https://daehwankimlab.github.io/hisat2/) and Blastn (https://blast.ncbi.nlm.nih.gov/Blast.cgi).

Analysis of Differentially Expressed mRNAs and miRNAs

For mRNAs, the expected number of fragments per kilobase of transcript sequences per million base pairs sequenced (FPKMs) was determined through RSEM (http://deweylab.github.io/RSEM/). A p-adjusted value of < 0.05 and an absolute value of log2 (fold change) ≥ 1.0 were set as the threshold for significant differential expression by using edgeR (http://www.bioconductor.org/packages/2.12/bioc/html/edgeR.html). For miRNAs, standardized transcripts per million clean tags values(TPM) were applied to known miRNAs by miRBase (miRBase 21 , http://www.mirbase.org/) [18, 19]. The novel miRNAs were predicted by miRDeep2 [20]. The expression data was analyzed using a model based on the negative binomial distribution for determining differential expression by DESeq2 [21]. The screening criteria for significantly expressed miRNAs: p-value < 0.05 and a fold change of ≥ 1.0.

GO Annotation and KEGG Pathway Analysis

The prediction of target genes of differentially expressed miRNAs was performed by miRanda [22]. Gene ontology (GO, http://www.geneontology.org/) and Kyoto Encyclopedia of Genes and Genomes (KEGG, https://www.genome.jp/kegg) databases were used to determine functions and metabolic pathways of differentially expressed miRNA-target genes. GO terms and KEGG pathways with p-values < 0.05 were considered significantly enriched.

Construction of Differentially Expressed miRNA-mRNA-Pathway Network

After target genes of differentially expressed miRNAs were identified, they were compared to differentially expressed mRNAs detected in SADS-CoV infection to obtain the pairs of miRNA-mRNA in network. Then mRNA-pathway pairs were defined by merging KEGG pathway analysis of miRNA-target genes and that of differentially expressed mRNAs. Finally, the miRNA-mRNA-pathway network was constructed based on miRNA-mRNA pairs and mRNA-pathway pairs using Cytoscape software (version 3.0, https://cytoscape.org/download.php).

Verification of RNA-Seq Data using qRT-PCR

A total of six genes including three miRNAshsa-miR-511-3p, hsa-miR-1323 and hsa-miR-181d-3p, and three mRNAs (MSTRG.21666.7, MSTRG.13726.11 and rna23915) were randomly selected for real-time qPCR validation. Total RNA was extracted from uninfected and infected Vero cells using TRIzol (Takara, Japan). cDNA was synthesized using miRNA First Strand cDNA Synthesis Kit (Sangon Biotech, China)with 5μg total RNA according to the manufacturer's instruction. Universal U6 primer F and universal PCR primer R were provided by miRNA First Strand cDNA Synthesis Kit (Sangon Biotech, China). The other primers were designed by Snap Gene 3.1.1 (Table **1**). The qRT-PCR was performed with the protocol of denaturation at 95℃ for 30s and 40 cycles at 95℃for 5s, 60℃for 30s, and finally a melting curve. Relative expressions of miRNAs and mRNAs were calculated through $2^{-\Delta\Delta Ct}$ equation. All values were normalized to the internal control U6 or glyceraldehyde-3-phosphate dehydrogenase (GAPDH) for miRNAs or mRNAs. Each reaction was performed in triplicate.

RESULES

Expression of mRNAs and miRNAs in Vero Cells after SADS-CoV Infection

Determination of miRNA/mRNA interactions could provide molecular insight about SADS-CoV infection mechanisms. In the present study, we examined the mRNAs and miRNAs profiles of infected and mock-infected Vero cells at 4hpi, 8hpi and 16hpi, respectively. The threshold for up- and down-regulated genes was a fold change of ≥1.0 and a p-value < 0.05.Results showed that there were 237(158 down, 79 up), 429(287 down, 142 up), 348(206 down, 142 up) differentially expressed mRNAs at 4hpi, 8hpi, 16hpi, respectively. MSTRG.23028.50 was the most down-regulated gene with 16.28-fold change, and MSTRG.27101.2 was the most up-regulated gene with 16.6-fold change. There were three genes, rna43709, MSTRG.11422.1and MSTRG.23025.13, which were detected with significantly differential expression at all three indicated time points. Rna43709 and MSTRG.23025.13 were down-regulated at 4hpi and 8hpi, while up-regulated at 16hpi. MSTRG.11422.1 was identified with down-regulation at three sampling time (Figure **1**). Compare to the mock-infected group, there were 40, 67, 88 known miRNAs that presented significant differences in expression at 4hpi, 8hpi, 16hpi, respectively. Results showed that hsa-miR-181d-3p was the most down-regulated miRNA with

Table 1: Primers for RT-qPCR Validation

Primers	Sequence(5'-3')
GAPDH-F	TGGACCTGACCTGCCGTCTG
GAPDH-R	CAGCGTCGAAGGTGGAAGAGTG
MSTRG.21666.7-F	CCAAGATTCACCAGGACACGAGAC
MSTRG.21666.7-R	TTTAGATTGCCCAGCCAGAAAGCC
MSTRG.13726.11-F	CGCCACCCTCTCCCTCCTTC
MSTRG.13726.11-R	TCTTCCAAGCCAATCAGCCAGTTC
rna23915-F	GTCAGCCACATCGGACACAACC
rna23915-R	GTCAGCCACATCGGACACAACC
hsa-miR-511-3p-F	ACGCGAATGTGTAGCAAAAGACAGA
hsa-miR-1323-F	CCGTCAAAACTGAGGGGCATTTTCT
hsa-miR-181d-3p-F	CCACCGGGGGATGAATGTCA

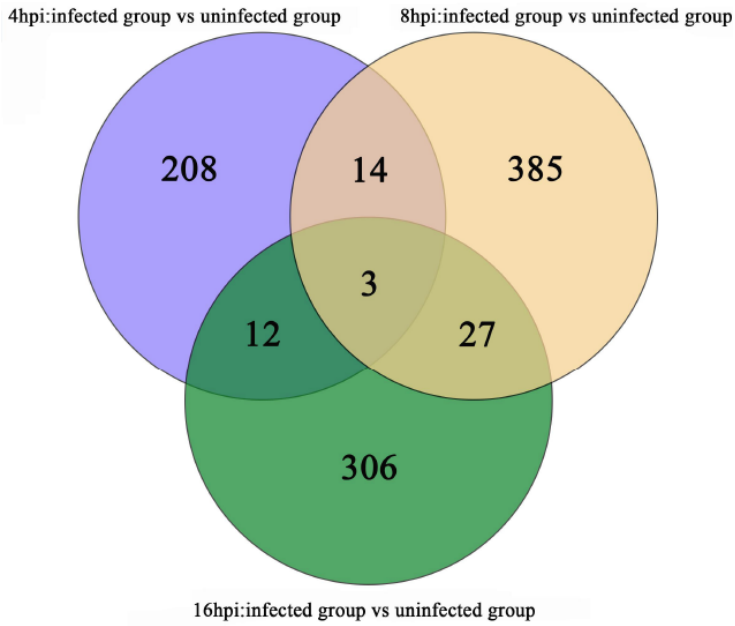

Figure 1: Identification of mRNAs during SADS-CoV infection. Common differentially expressed genes in three stages. 4hpi: infected group vs uninfected group; 8hpi: infected group vs uninfected group; 16hpi: infected group vs uninfected group.

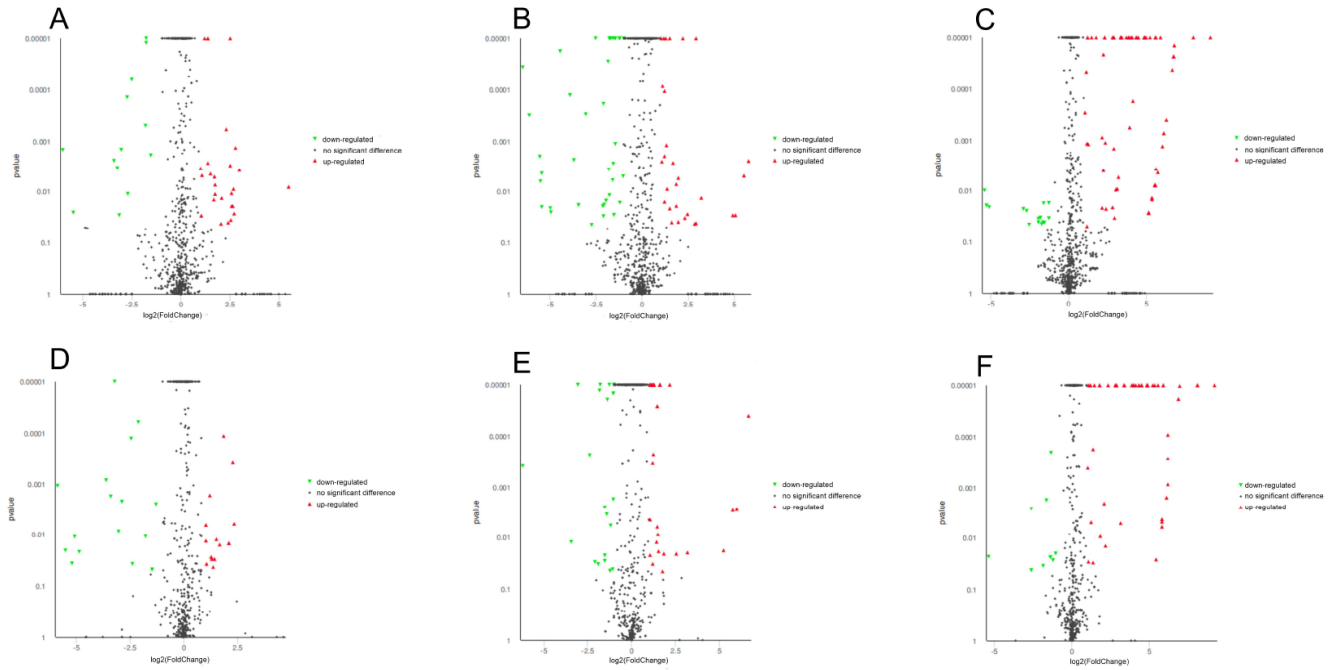

Figure 2: Visualization of differentially expressed miRNAs with Volcano-plots. **A**, **B** and **C** represent known miRNAs at 4hpi, 8hpi, 16hpi, respectively. **D**, **E** and **F** represent novel miRNAs at 4hpi, 8hpi, 16hpi, respectively. Abscissa, the fold changes value of the differentially expressed miRNAs between the two samples. Ordinate, *p*-value. Each dot in the figure represents a specific miRNA. Red, up-regulation. Green, down-regulation. Black, no significant difference.

6.49-fold change, and hsa-miR-31-5pwas the most up-regulated miRNA with 9.14-foldchange. MicroRNA hsa-miR-146a-3p was the only one that showed significant differences in all three sampling stages, and with up-regulation. We also identified some novel miRNAs, and there were 32, 53, 65 novel miRNAs that showed significant differences at 4hpi, 8hpi, 16hpi, respectively (Figure **2**).

Target Gene Prediction and Enrichment Analysis

The miRNAs performed their functions through the post-transcriptional regulation of their target genes. The

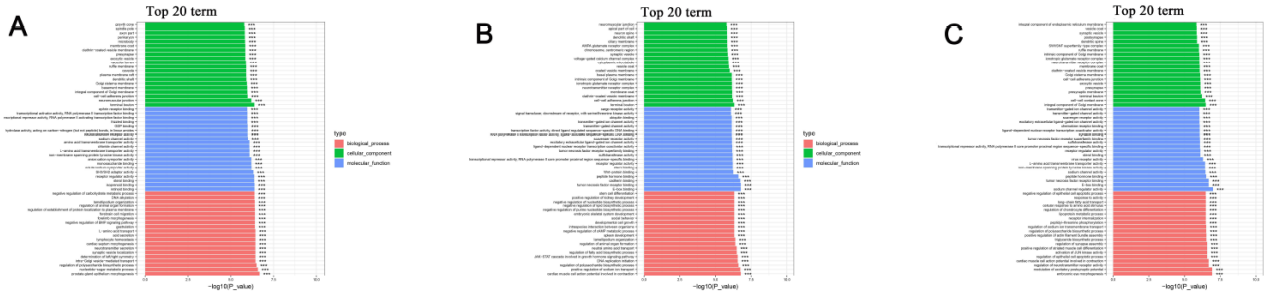

Figure 3: The top 20 GO terms of target genes. **A**, **B** and **C** represent 4hpi, 8hpi, 16hpi, respectively. Different color represents different type. Green, cellular components. Blue, molecular function. Red, biological process. ***, $p<0.001$.

functional study of miRNA is actually the functional study of target genes. The prediction of miRNA target genes was performed by miRanda. GO annotation revealed that genes targeted by differentially expressed miRNAs were enriched in three mainly modules including biological process, cellular components and molecular function after SADS-CoV infection. GO annotation of miRNA target genes indicated that 3,288, 3,471 and 3,533 GO terms were significantly enriched at 4hpi, 8hpi, 16hpi, respectively. In terms of cellular components, terminal bouton, cell-cell adherens junction and integral component of Golgi membrane were involved all three stages. To the biological process, prostate gland epithelium morphogenesis, cardiac muscle cell action potential involved in contraction and embryonic eye morphogenesis were detected with relatively more miRNA target genes at the early, middle, late stage, respectively. For the molecular function, target genes were mainly associated with transport activity, including sodium channel activity, chloride channel activity, ion channel activity. Tumor necrosis factor receptor superfamily binding and tumor necrosis factor receptor binding were detected at the middle and late stage, indicating that miRNA target genes were related to cancer diseases (Figure **3**).

KEGG pathway analysis of miRNA target genes indicated that 62, 61, 51 pathways were significantly enriched at 4hpi, 8hpi, 16hpi, respectively. In three stages, top 2 pathways were Cytokine-cytokine receptor interaction and Neuroactive ligand-receptor interaction. And these three periods shared 49 common pathways with different levels of significance. Target genes of miRNAs were mainly active in pathways related to environmental information processing, cellular processes, organismal systems and human diseases for three sampling time points. Among those four categories, environmental information processing and organismal systems enriched most miRNA target genes. SADS-CoV infection induced immunology responses of the host cell. For examples, B cell receptor signaling pathway, toll-like receptor signaling pathway and inflammatory mediator regulation of TRP channels were identified. In addition, cancer related chemokine signaling pathway, MAPK signaling pathway, cAMP signaling pathway, and cardiovascular disease related TNF signaling pathway were also found with differentially expressed target genes of miRNAs (Figure **4**). These results suggested that SADS-CoV infection could influence miRNA expression in infected cells, while differentially expressed miRNAs may further affect gene expression and metabolic processes.

Functional Network of Differentially Expressed miRNAs and Target Genes

To investigate the effect of differentially expressed miRNAs on target mRNAs, the network of miRNA-mRNA-pathway after SADS-CoV infection was examined. Results showed that the network was composed of 17 mRNAs, 93miRNAs and 34 pathways nodes. And there were 15miRNAs-3 target genes, 39 miRNAs-8 target genes, and 44miRNAs-8 target genes involved at 4hpi, 8hpi and 16hpi, respectively. The number of correspondingly pathways involved with these mRNAs and miRNAs at three different infection stages were 5, 13 and 20, respectively.

At 4hpi of SADS-CoV infection in Vero cells, SIRPA_B1_G and TUBA were two main mRNAs, which were down-regulated and up-regulated by six and eight different miRNAs, respectively. TUBA was also significantly up-regulated in the mid-stage of infection. KRAB was another central mRNA, significantly down-regulated in the mid- and late-stage of infection. Four pathways including pathogenic Escherichia coli infection, phagosome, apoptosis and gap junction, were all detected in the early and middle stages, suggesting their important roles in SADS-CoV infection.

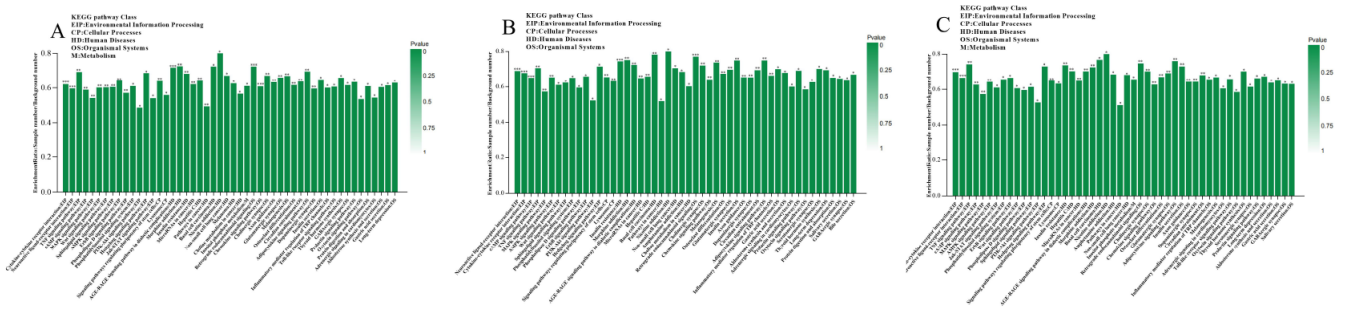

Figure 4: KEGG pathway enrichment analysis of target genes. **A**, **B** and **C** represent the enrichment pathway of genes at 4hpi, 8hpi, 16hpi, respectively. Each column in the figure is a pathway and the color depth is proportional to significance. Abscissa, the different pathways. Ordinate, enrichment ratio. The classification description is shown in the upper left corner. The color gradient on the right side represents the size of *p*-value. *, $p < 0.05$.**, $p < 0.01$.***, $p < 0.001$. The signaling pathway shown in the figure that represents in the top 50 *p*-value ranking.

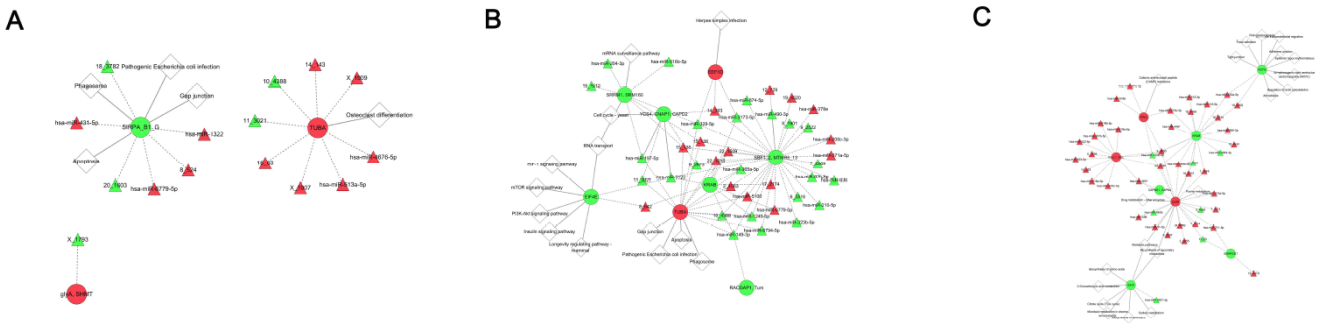

Figure 5: The miRNA-mRNA-pathway network. **A**, the early stage of infection. **B**, the middle stage of infection. **C**, the late stage of infection. Triangle, miRNA. Circle, mRNA. Rectangle, pathway. Green, down-regulation. Red, up-regulation.

While in the late stage of infection, metabolic pathways, focal adhesion, tight junction, adherens junction and so on were identified (Figure **5**).

Validation of Selected miRNAs and mRNAs in SADS-CoV Infection by qRT-PCR

The RNA-Seq analysis indicated that the expression level of miRNAs and mRNAs significantly changed in the infected group compared with that in the uninfected group. To verify the authenticity of RNA-Seq data, 6 genes includinghsa-miR-511-3p, hsa-miR-1323, hsa-miR-181d-3p, MSTRG.21666.7, MSTRG.13726.11 and rna23915 were randomly selected for verification. Validation results of qRT-PCR were consistent with that of the RNA-Seq, which indicated that data of RNA-Seq was reliable (Figure **6**).

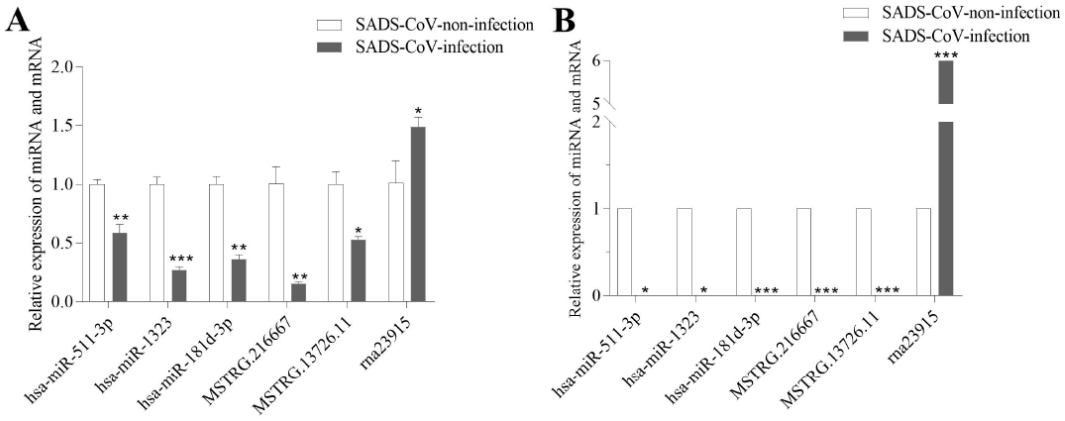

Figure 6: Verification of RNA-Seq results. Six differentially expressed genes were randomly selected for real-time qRT-PCR to verify whether their expression levels were consistent with the RNA-Seq results. **A**, the expression verification results of six genes (hsa-miR-511-3p, hsa-miR-1323, hsa-miR-181d-3p, MSTRG.21666.7, MSTRG.13726.11, rna23915). **B**, the RNA-Seq results of these genes. *, $p<0.05$.**, $p<0.01$.***, $p<0.001$.

DISCUSSION

SADS-CoV is a novel coronavirus that has brought losses in pig industry [3, 4]. Studies on miRNA expression profiles and regulations of miRNAs during viral infection could help better understanding the infection mechanisms of SADS-CoV. In this study, SADS-CoV-infected Vero cells were chosen as the research subject, and we preliminarily explored the miRNA molecular regulatory pathways during infection with the virus. Our results showed that the aberrant expression of microRNAs including hsa-miR-149-3p, hsa-miR-431-5p and hsa-miR-1322 may active pathways including pathogenic Escherichia coli infection, phagosome, apoptosis and gap junction by targeting TUBA or SIRPA_B1_G after SADS-CoV infection. Research indicated that hsa-miR-149-3p may result in up-regulation of genes in pathways related to coxsackievirus A16 (CVA16) and further causing clinical symptoms [23]. Our data showed that after SADS-CoV infection, hsa-miR-149-3p was down differentially expressed, but induced up-expression of TUBA. It was suggested that hsa-miR-431-5p was involved in diffuse large B-cell lymphoma (DLBCL) pathogenesis by regulating FYN (a tumor suppressor in prostate cancer) expression [24]. Some scholars found that miR-1322 played an oncogenic role in initiation and progression of esophageal squamous cell carcinoma (ESCC) by regulating ECRG2 (an esophageal cancer related tumor suppressor) [25]. Combined our results and these findings, it indicated that the three miRNAs regulate more genes and participate in different pathways, which deserve more studies.

The network of miRNA-mRNA-pathway studied here revealed that with the extension of SADS-CoV infection, more miRNAs, target genes and involved pathways were detected. We have found that KRAB was down-regulated in mid- and late-stage, and it was negatively regulated by hsa-miR-6779-5p at mid-stage or by hsa-miR-512-3p, has-miR-4461 and other microRNAs at late-stage. Research has shown that KRAB is related to cancer. KRAB-containing zinc finger proteins (ZFPs) represent one of the largest families of DNA-binding proteins, and these proteins may play an oncogenic role during carcinogenesis [26, 27]. For example, ZFP82 was a tumor suppressor and it was down-regulated in esophageal squamous cell carcinoma, and the expression of ZFP82 suppressed cell function and cells apoptosis. The spalt-like transcription factor 1 (SALL1) gene is a member of KRAB-ZFPs and has been shown to modulate the onset and progression of human tumors, overexpression of ZFP57/ZNF382 could inhibit the proliferation of breast cancer cells or ESCC pathogenesis by inhibiting the Wnt/beta-catenin pathway [28-31]. Therefore, the down-regulation of KRAB may activate the cancer-related pathway, while studies on related-miRNAs, such as hsa-miR-6779-5p, has-miR-4461 are still limited, and then the relationship between them are need to be explored.

KEGG analysis showed that PI3K-Akt signaling pathway was significantly enriched in three stages, and the network analysis also identified this pathway. We found that this pathway was related to a down regulated gene, eIF4E in the network of 8hpi.Research indicated that eIF4E was involved in miR-15a-induced inhibition of cell proliferation and invasion of RCC cells which may be mediated by the activation of the PI3K/AKT/mTOR signaling pathway [32]. Over expression of eIF4E has been found in cancer activities, and inhibition of eIF4E expression mayinduce cell apoptosis [33, 34]. Our results suggested that downregulation of eIF4E may promote cell apoptosis by mediating by PI3K-Akt signaling pathway. Pathogenic Escherichia coli infection was another important pathway, which was enriched in the early and middle stages after SADS-CoV infection. SADS-CoV is a diarrhoea virus, and its secondary bacterial infection was one of the reasons for mortality. The research about pathogenic Escherichia coli infection pathway was limited, but it has possibility with secondary bacterial infection, and needs further studies.

CONCLUSIONS

In this study, we provide the first analysis of differentially expressed miRNAs and mRNAs after SADS-CoV infection in Vero cells. We constructed a miRNA-mRNA-pathway network, which indicated that differentially expressed miRNA involved in PI3K-Akt signaling pathway and pathogenic Escherichia coli infection during SADS-CoV infection. This study provides insights into the relationships between miRNAs and SADS-CoV infection, which would help to address miRNA functions in immune escape used by SADS-CoV.

FUNDING

This work was supported by the Science and Technology Program of Guangzhou City of China (No. 201904010433), and the Research and Extension of

Major Animal Epidemic Prevention and Control Technologies in the Strategic Project of Rural Revitalization of Guangdong Agricultural Department of China (Building Modern Agricultural System) (2018-2020). The funders did not play any role in the design, conclusions or interpretation of the study.

REFERENCE

[1] Gong L, Li J, Zhou Q, Xu Z, Chen L, Zhang Y, Xue C, Wen Z, Cao Y. A New Bat-HKU2-like Coronavirus in Swine, China, 2017. Emerging Infectious Diseases 2017; 23(9). https://doi.org/10.3201/eid2309.170915

[2] Pan Y, Tian X, Qin P, Wang B, Zhao P, Yang YL, Wang L, Wang D, Song Y, Zhang X, *et al.* Discovery of a novel swine enteric alphacoronavirus (SeACoV) in southern China. Veterinary Microbiology 2017; 211: 15-21. https://doi.org/10.1016/j.vetmic.2017.09.020

[3] Zhou P, Fan H, Lan T, Yang XL, Shi WF, Zhang W, Zhu Y, Zhang YW, Xie QM, Mani S, *et al.* Fatal swine acute diarrhoea syndrome caused by an HKU2-related coronavirus of bat origin. Nature 2018; 556(7700): 255-258. https://doi.org/10.1038/s41586-018-0010-9

[4] Zhou L, Sun Y, Lan T, Wu R, Chen J, Wu Z, Xie Q, Zhang X, Ma J. Retrospective detection and phylogenetic analysis of swine acute diarrhoea syndrome coronavirus in pigs in southern China. Transboundary and Emerging Diseases 2019; 66(2): 687-695. https://doi.org/10.1111/tbed.13008

[5] Li K, Li H, Bi Z, Gu J, Gong W, Luo S, Zhang F, Song D, Ye Y, Tang Y. Complete Genome Sequence of a Novel Swine Acute Diarrhea Syndrome Coronavirus, CH/FJWT/2018, Isolated in Fujian, China, in 2018. Microbiology Resource Announcements 2018; 7(22). https://doi.org/10.1128/MRA.01259-18

[6] Zhou L, Li QN, Su JN, Chen GH, Wu ZX, Luo Y, Wu RT, Sun Y, Lan T, Ma JY. The re-emerging of SADS-CoV infection in pig herds in Southern China. Transboundary and Emerging Diseases 2019; 66(5): 2180-2183. https://doi.org/10.1111/tbed.13270

[7] Bartel DP. MicroRNAs: Target Recognition and Regulatory Functions. Cell 2009; 136(2): 215-233. https://doi.org/10.1016/j.cell.2009.01.002

[8] Huang J, Lang Q, Li X, Xu Z, Zhu L, Zhou Y. [MicroRNA Expression Profiles of Porcine Kidney 15 Cell Line Infected with Porcine Epidemic Diahorrea Virus]. Bing Du Xue Bao 2016; 32(4): 465-471.

[9] Cao LY, Ge XY, Gao Y, Ren YD, Ren XF, Li GX. Porcine epidemic diarrhea virus infection induces NF-kappa B activation through the TLR2, TLR3 and TLR9 pathways in porcine intestinal epithelial cells. Journal of General Virology 2015; 96: 1757-1767. https://doi.org/10.1099/vir.0.000133

[10] Zheng HQ, Xu L, Liu YZ, Li C, Zhang L, Wang T, Zhao D, Xu XG, Zhang YM. MicroRNA-221-5p Inhibits Porcine Epidemic Diarrhea Virus Replication by Targeting Genomic Viral RNA and Activating the NF-kappa B Pathway. International Journal of Molecular Sciences 2018; 19(11). https://doi.org/10.3390/ijms19113381

[11] Ma Y, Wang C, Xue M, Fu F, Zhang X, Li L, Yin L, Xu W, Feng L, Liu P. The Coronavirus Transmissible Gastroenteritis Virus Evades the Type I Interferon Response through IRE1alpha-Mediated Manipulation of the MicroRNA miR-30a-5p/SOCS1/3 Axis. Journal of Virology 2018; 92(22). https://doi.org/10.1128/JVI.00728-18

[12] Ma X, Zhao X, Zhang Z, Guo J, Guan L, Li J, Mi M, Huang Y, Tong D. Differentially expressed non-coding RNAs induced by transmissible gastroenteritis virus potentially regulate inflammation and NF-kappaB pathway in porcine intestinal epithelial cell line. BMC Genomics 2018; 19(1): 747. https://doi.org/10.1186/s12864-018-5128-5

[13] Zhao X, Bai X, Guan L, Li J, Song X, Ma X, Guo J, Zhang Z, Du Q, Huang Y, *et al.* microRNA-4331 Promotes Transmissible Gastroenteritis Virus (TGEV)-induced Mitochondrial Damage Via Targeting RB1, Upregulating Interleukin-1 Receptor Accessory Protein (IL1RAP), and Activating p38 MAPK Pathway In vitro. Mol Cell Proteomics 2018; 17(2): 190-204. https://doi.org/10.1074/mcp.RA117.000432

[14] Zhao X, Song X, Bai X, Fei N, Huang Y, Zhao Z, Du Q, Zhang H, Zhang L, Tong D. miR-27b attenuates apoptosis induced by transmissible gastroenteritis virus (TGEV) infection via targeting runt-related transcription factor 1 (RUNX1). PeerJ 2016; 4: e1635. https://doi.org/10.7717/peerj.1635

[15] Li N, Du TF, Yan YH, Zhang AK, Gao JM, Hou GP, Xiao SQ, Zhou EM. MicroRNA let-7f-5p Inhibits Porcine Reproductive and Respiratory Syndrome Virus by Targeting MYH9. Scientific Reports 2016; 6. https://doi.org/10.1038/srep34332

[16] Xiao SQ, Du TF, Wang X, Ni HB, Yan YH, Li N, Zhang C, Zhang AK, Gao JM, Liu HL, *et al.* MiR-22 promotes porcine reproductive and respiratory syndrome virus replication by targeting the host factor HO-1. Veterinary Microbiology 2016; 192: 226-230. https://doi.org/10.1016/j.vetmic.2016.07.026

[17] Xiao SQ, Wang X, Ni HB, Li N, Zhang AK, Liu HL, Pu FX, Xu LL, Gao JM, Zhao Q, *et al.* MicroRNA miR-24-3p Promotes Porcine Reproductive and Respiratory Syndrome Virus Replication through Suppression of Heme Oxygenase-1 Expression. Journal of Virology 2015; 89(8): 4494-4503. https://doi.org/10.1128/JVI.02810-14

[18] Zhou LA, Chen JH, Li ZZ, Li XX, Hu XD, Huang Y, Zhao XK, Liang CZ, Wang Y, Sun LA, *et al.* Integrated Profiling of MicroRNAs and mRNAs: MicroRNAs Located on Xq27.3 Associate with Clear Cell Renal Cell Carcinoma. PloS One 2010; 5(12). https://doi.org/10.1371/journal.pone.0015224

[19] Kozomara A, Griffiths-Jones S. miRBase: annotating high confidence microRNAs using deep sequencing data. Nucleic Acids Research 2014; 42(D1): D68-D73. https://doi.org/10.1093/nar/gkt1181

[20] Friedlander MR, Mackowiak SD, Li N, Chen W, Rajewsky N. miRDeep2 accurately identifies known and hundreds of novel microRNA genes in seven animal clades. Nucleic Acids Research 2012; 40(1): 37-52. https://doi.org/10.1093/nar/gkr688

[21] Anders S, Huber W. Differential expression analysis for sequence count data. Genome Biol 2010; 11(10). https://doi.org/10.1186/gb-2010-11-10-r106

[22] Enright AJ, John B, Gaul U, Tuschl T, Sander C, Marks DS. MicroRNA targets in Drosophila. Genome Biol 2003; 5(1): R1. https://doi.org/10.1186/gb-2003-5-1-r1

[23] Jin J, Li R, Jiang C, Zhang R, Ge X, Liang F, Sheng X, Dai W, Chen M, Wu J, *et al.* Transcriptome analysis reveals dynamic changes in coxsackievirus A16 infected HEK 293T cells. BMC Genomics 2017; 18(Suppl 1): 933. https://doi.org/10.1186/s12864-016-3253-6

[24] Meng Y, Quan L, Liu A. Identification of key microRNAs associated with diffuse large B-cell lymphoma by analyzing serum microRNA expressions. Gene 2018; 642: 205-211. https://doi.org/10.1016/j.gene.2017.11.022

[25] Zhang T, Zhao D, Wang Q, Yu X, Cui Y, Guo L, Lu SH. MicroRNA-1322 regulates ECRG2 allele specifically and acts as a potential biomarker in patients with esophageal

squamous cell carcinoma. Molecular Carcinogenesis 2013; 52(8): 581-590. https://doi.org/10.1002/mc.21880

[26] Shi H, Strogantsev R, Takahashi N, Kazachenka A, Lorincz MC, Hemberger M, Ferguson-Smith AC. ZFP57 regulation of transposable elements and gene expression within and beyond imprinted domains. Epigenetics Chromatin 2019; 12(1): 49. https://doi.org/10.1186/s13072-019-0295-4

[27] Machnik M, Cylwa R, Kielczewski K, Biecek P, Liloglou T, Mackiewicz A, Oleksiewicz U. The expression signature of cancer-associated KRAB-ZNF factors identified in TCGA pan-cancer transcriptomic data. Mol Oncol 2019; 13(4): 701-724. https://doi.org/10.1002/1878-0261.12407

[28] Ye L, Xiang T, Fan Y, Zhang D, Li L, Zhang C, He X, Xiang Q, Tao Q, Ren G. The 19q13 KRAB Zinc-finger protein ZFP82 suppresses the growth and invasion of esophageal carcinoma cells through inhibiting NF-kappaB transcription and inducing apoptosis. Epigenomics 2019; 11(1): 65-80. https://doi.org/10.2217/epi-2018-0092

[29] Chi D, Zhang W, Jia Y, Cong D, Hu S. Spalt-Like Transcription Factor 1 (SALL1) Gene Expression Inhibits Cell Proliferation and Cell Migration of Human Glioma Cells Through the Wnt/beta-Catenin Signaling Pathway. Med Sci Monit Basic Res 2019; 25: 128-138. https://doi.org/10.12659/MSMBR.915067

[30] Zhang C, Xiang T, Li S, Ye L, Feng Y, Pei L, Li L, Wang X, Sun R, Ren G, *et al.* The novel 19q13 KRAB zinc-finger tumour suppressor ZNF382 is frequently methylated in oesophageal squamous cell carcinoma and antagonises Wnt/beta-catenin signalling. Cell Death & Disease 2018; 9(5): 573. https://doi.org/10.1038/s41419-018-0604-z

[31] Shen S, Wu Y, Chen J, Xie Z, Huang K, Wang G, Yang Y, Ni W, Chen Z, Shi P, *et al.* CircSERPINE2 protects against osteoarthritis by targeting miR-1271 and ETS-related gene. Annals of the Rheumatic Diseases 2019. https://doi.org/10.1136/annrheumdis-2018-214786

[32] Li G, Chong T, Xiang X, Yang J, Li H. Downregulation of microRNA-15a suppresses the proliferation and invasion of renal cell carcinoma via direct targeting of eIF4E. Oncology Reports 2017; 38(4): 1995-2002. https://doi.org/10.3892/or.2017.5901

[33] Campbell L, Jasani B, Griffiths DFR, Gumbleton M. Phospho-4e-BP1 and eIF4E overexpression synergistically drives disease progression in clinically confined clear cell renal cell carcinoma. Am J Cancer Res 2015; 5(9): 2838-2848.

[34] Ilic N, Utermark T, Widlund HR, Roberts TM. PI3K-targeted therapy can be evaded by gene amplification along the MYC-eukaryotic translation initiation factor 4E (eIF4E) axis. Proc Natl Acad Sci USA 2011; 108(37): E699-U607. https://doi.org/10.1073/pnas.1108237108

Received on 10-03-2020 Accepted on 02-06-2020 Published on 10-06-2020

DOI: https://doi.org/10.12970/2310-0796.2020.08.06